

On the Use of Torque Measurement in Centroidal State Estimation

Shahram Khorshidi¹, Ahmad Gazar¹, Nicholas Rotella², Maximilien Naveau³,
Ludovic Righetti^{1,4}, Majid Khadiv¹

Abstract—State of the art legged robots are either capable of measuring torque at the output of their drive systems, or have transparent drive systems which enable the computation of joint torques from motor currents. In either case, this sensor modality is seldom used in state estimation. In this paper, we propose to use joint torque measurements to estimate the centroidal states of legged robots. To do so, we project the whole-body dynamics of a legged robot into the nullspace of the contact constraints, allowing expression of the dynamics independent of the contact forces. Using the constrained dynamics and the centroidal momentum matrix, we are able to directly relate joint torques and centroidal states dynamics. Using the resulting model as the process model of an Extended Kalman Filter (EKF), we fuse the torque measurement in the centroidal state estimation problem. Through real-world experiments on a quadruped robot with different gaits, we demonstrate that the estimated centroidal states from our torque-based EKF drastically improve the estimation of these quantities compared to direct computation.

I. INTRODUCTION

State estimation for legged robots plays a crucial role in the successful application of modern state feedback controllers to this domain. The estimation problem is especially difficult for legged robots, as they are inherently underactuated and experience uncertain, intermittent contacts with the environment during motion. Furthermore, their dynamics are highly nonlinear, which makes the design of estimators nontrivial.

The majority of legged robot estimation works to date have focused on base state estimation. This problem is particularly difficult for floating base systems, as the base pose cannot be measured directly. One of the most widely used choices for base state estimation is the Extended Kalman Filter (EKF) [1], [2], [3]. While there have been recent attempts to use more advanced approaches based on the use of factor graphs [4] and invariant Kalman Filters [5], the EKF framework is commonly used due to its compromise between simplicity, efficiency, and performance [6].

For base state estimation, most works have fused Inertial Measurement Unit (IMU) data with leg odometry to estimate the base position and velocity as well as its orientation [1], [2]. Furthermore, to compensate for the drift of the unobservable base position while simultaneously mapping the environment, sensor modalities like lidar and cameras are often added [3], [6].

Force measurement at the endeffectors of legged robots is another useful source of information that can be used to better estimate [7] and handle contact switch events [8], [9] as well as aid in estimation of the centroidal states [10], [4]. However, since it is highly important for legged robots to have low leg inertia for agile movements, using sensorized feet [9] can drastically degrade the range of dynamic movements they can perform, especially for quadrupeds. Thus, most of works in this area first estimate the contact forces without direct sensing, and then use the estimated forces for state estimation [8], [4].

While legged robots often lack endeffector force sensing, they commonly boast joint torque sensing. In this work, we propose to fuse joint torque measurements with the nonlinear dynamic model in the EKF framework to estimate the centroidal states – namely, the center of mass position and momenta – of a legged robot. We argue that since most of the state-of-the-art quadrupedal [11], [12], [13] and bipedal [14], [15], [16] platforms have the capability to measure or estimate joint torque, this sensing modality can be used to perform centroidal state estimation regardless of contact force measurement capabilities. Model-based centroidal state computations are usually very noisy due to noise in measured joint velocities, and low-pass filtering can introduce delays on the order of tens of milliseconds; such large delays can destabilize high rate controllers [10]. By using joint torque measurements for centroidal estimation, we can avoid this issue without necessitating contact force sensing.

A. Contributions

The main contributions of this work are as follows:

- We propose an EKF-based framework which fuses the whole body dynamics of a legged robot projected into the nullspace of the contact constraints with joint torque measurements in order to perform centroidal state estimation. To the best of our knowledge, this is the first time that this sensing modality has been used to estimate the centroidal states of a legged robot. Notably, the proposed framework is general enough to be used on any legged robot, not just a quadruped.

¹Max-Planck Institute for Intelligent Systems, Tübingen, Germany {skhorshidi, agazar, lrighetti, mkhadiv}@tuebingen.mpg.de

²Seegrid Corporation, Pittsburgh, USA
nicholas.rotella@gmail.com

³Centre National de la Recherche Scientifique (CNRS), Laboratoire d'Analyse et d'Architecture des Systemes (LAAS), Toulouse mnaveau@laas.fr

⁴Tandon School of Engineering, New York University, USA ludovic.righetti@nyu.edu

This work was supported by the Max-Planck Institute for Intelligent Systems' Grassroots program (M10338 and M10343), New York University, the European Union's Horizon 2020 research and innovation program (grant agreement 780684) and the National Science Foundation (CMMI-1825993).

- We demonstrate, through an extensive set of experiments with different gaits on the real quadruped robot Solo12 [13], that the use of torque measurements provides accurate centroidal state estimation with minimal noise and time delay.

B. Notation

Throughout the paper, we use small letters to specify scalars and scalar-valued functions, bold small letters for vectors and vector-valued functions, and capital letters for matrices.

II. FUNDAMENTALS

The dynamics of a floating-base system can be written as

$$M(\mathbf{q})\dot{\mathbf{v}} + \mathbf{n}(\mathbf{q}, \mathbf{v}) = B\boldsymbol{\tau} + J_c^T \boldsymbol{\lambda}, \quad (1)$$

where $M \in \mathbb{R}^{(n+6) \times (n+6)}$ is the mass-inertia matrix, $\mathbf{q} \in SE(3) \times \mathbb{R}^n$ denotes the configuration space, $\mathbf{v} \in \mathbb{R}^{n+6}$ encodes the vector of generalized velocities (or more precisely quasi-velocities), and $\mathbf{n} \in \mathbb{R}^{n+6}$ is a concatenation of non-linear terms including centrifugal, Coriolis and gravitational effects. $B \in \mathbb{R}^{(n+6) \times n}$ is a selection matrix that separates the actuated and unactuated Degrees of Freedom (DoFs), $\boldsymbol{\tau} \in \mathbb{R}^n$ is the vector of actuating torques, $J_c \in \mathbb{R}^{3m \times (n+6)}$ is the Jacobian of m feet in contact, and finally $\boldsymbol{\lambda} \in \mathbb{R}^{3m}$ is the vector of contact forces (here we assume point-contact feet for quadrupeds, however all results hold for humanoids with flat feet as well).

A. Motion and Constraint Dynamics

Assuming that the foot contacts are rigid, and using the orthogonal projection operator $N = I - J_c^\dagger J_c$ (where † stands for the Moore-Penrose inverse) which projects into the nullspace of the contact Jacobian, we can divide (1) into the following set of equations [17]

$$NM(\mathbf{q})\dot{\mathbf{v}} + N\mathbf{n}(\mathbf{q}, \mathbf{v}) = NB\boldsymbol{\tau}, \quad (2a)$$

$$(I - N)(M(\mathbf{q})\dot{\mathbf{v}} + \mathbf{n}(\mathbf{q}, \mathbf{v})) = (I - N)B\boldsymbol{\tau} + J_c^T \boldsymbol{\lambda}. \quad (2b)$$

Equation (2a) encodes the dynamics of the robot motion independent of the constraint forces, while (2b) yields the dynamics of the system in the contact constraint space [17]. In other words, $NB\boldsymbol{\tau}$ is used to move the system on a desired trajectory without violating the contact constraint, while $(I - N)B\boldsymbol{\tau}$ preserves the stationary contact. Interestingly, as (2a) is independent of contact forces, we can use it to relate the measured torque to the joint accelerations without knowledge of the contact forces. This is especially useful for agile legged robots whose endeffectors are often not equipped with contact force/torque sensors.

Since the feet in contact are assumed stationary, we can write down the following constraint and differentiate both sides with respect to time, yielding

$$(I - N)\mathbf{v} = \mathbf{0} \Rightarrow (I - N)\dot{\mathbf{v}} = \dot{N}\mathbf{v} \quad (3)$$

Defining the constraint-consistent mass-inertia matrix as $M_c = NM + I - N$ and substituting it along with (3) into (2a), we have

$$M_c(\mathbf{q})\dot{\mathbf{v}} - \dot{N}\mathbf{v} + N\mathbf{n}(\mathbf{q}, \mathbf{v}) = NB\boldsymbol{\tau}. \quad (4)$$

Now, we can invert M_c and solve the constraint-consistent equations of motion for $\dot{\mathbf{v}}$ to yield

$$\dot{\mathbf{v}} = M_c^{-1}(\dot{N}\mathbf{v} - N\mathbf{n} + NB\boldsymbol{\tau}). \quad (5)$$

B. Relation Between Joint Torques and Centroidal States

Denoting the centroidal momentum vector by $\mathbf{h}_G \in \mathbb{R}^6$, we can write down its relation with generalized velocities using

$$\mathbf{h}_G = [\mathbf{l}, \mathbf{k}]^T = A_G(\mathbf{q})\mathbf{v}, \quad (6)$$

where $A_G(\mathbf{q})$ is the centroidal momentum matrix [18]. Taking the derivative of (6) with respect to time yields

$$\dot{\mathbf{h}}_G = A_G(\mathbf{q})\dot{\mathbf{v}} + \dot{A}_G(\mathbf{q})\mathbf{v}. \quad (7)$$

Substituting (5) into (7), we have

$$\dot{\mathbf{h}}_G = A_G(M_c^{-1}(\dot{N}\mathbf{v} - N\mathbf{n} + NB\boldsymbol{\tau})) + \dot{A}_G\mathbf{v}. \quad (8)$$

Assuming that \mathbf{q}, \mathbf{v} are known using encoder measurements and base state estimation, we can simplify the momentum dynamics as

$$\dot{\mathbf{h}}_G = A(\mathbf{q}, \mathbf{v})\boldsymbol{\tau} + \mathbf{b}(\mathbf{q}, \mathbf{v}). \quad (9)$$

where

$$A(\mathbf{q}, \mathbf{v}) = A_G M_c^{-1} NB \quad (10a)$$

$$\mathbf{b}(\mathbf{q}, \mathbf{v}) = A_G M_c^{-1}(\dot{N}\mathbf{v} - N\mathbf{n}) + \dot{A}_G\mathbf{v}. \quad (10b)$$

III. ESTIMATION PROBLEM

We wish to estimate the centroidal states $\mathbf{x} = [\mathbf{c}, \mathbf{l}, \mathbf{k}]$ using joint torque measurements and the above momentum dynamics. The process model is

$$\begin{aligned} \dot{\mathbf{c}} &= \frac{1}{m}\mathbf{l} \\ [\dot{\mathbf{l}}, \dot{\mathbf{k}}]^T &= A\boldsymbol{\tau} + \mathbf{b} \end{aligned} \quad (11)$$

where \mathbf{c} is the center of mass (CoM) position and \mathbf{l} and \mathbf{k} are the linear and angular components of centroidal momentum, respectively. The measurement model is simply $\mathbf{y} = [\mathbf{c}, \mathbf{l}, \mathbf{k}]$. These values are computed using the results of base state estimation, measured generalized joint states, kinematics, and inertial properties of the robot. Specifically, we use (6) to compute the momenta while the CoM is computed using the estimated base state and joint measurements as

$$\mathbf{c} = \mathbf{g}(\mathbf{q}) \quad (12)$$

As shown in [10], although the centroidal states can be computed directly, they are subject to considerable noise and modeling errors. By fusing the computed states with a torque-based process model, we similarly obtain low-noise estimates with minimal delay, suitable for high-bandwidth control.

Remark 1: It is important to note that centroidal state estimation is performed under the assumption that a separate base state estimator provides estimates of the base pose and velocity. Also, for both base and centroidal state estimation, we need a contact detection mechanism for each foot. Hence, one might ask if we need already to estimate contact forces for contact estimation, then why not use a centroidal state estimator which is based on force (for instance, [10]) which would render the process model much simpler compared to (11). The answer to this question is threefold: 1) contact detection is normally performed by setting a threshold only on the *estimated normal force*, separately for each leg, and neglecting the dynamics. This force is not accurate enough to be used in the centroidal state estimation problem. 2) Instead of using the whole-body dynamics to estimate forces and then use the resulting forces to estimate the centroidal states, our approach in this paper does both in one stage. 3) Many legged robots are endowed with binary contact sensors at their endeffectors [13], [14] that can directly detect contact events, hence there is no need to estimate endeffector forces.

A. Extended Kalman Filtering

For the sake of simplicity and numerical efficiency, we choose to implement our estimator as an Extended Kalman Filter (EKF). The EKF estimates the mean μ and the error covariance P over the state x_k , where both process and measurement models are corrupted by additive zero-mean Gaussian noise. The stochastic system in discrete form is

$$x_k = f(x_{k-1}, u_{k-1}) + w_k \quad (13)$$

$$z_k = h(x_k) + v_k \quad (14)$$

where the input $u_k = \tau_k$ is the vector of joint torques and z_k is the measurement. The process noise $w_k \sim \mathcal{N}(0, Q_k)$ and measurement noise $v_k \sim \mathcal{N}(0, R_k)$ are parameterized by the corresponding covariance matrices Q_k R_k . These matrices constitute the main tuning parameters of the filter. Note that the process noise is chosen to be purely additive (rather than based on the uncertainty in torque sensing) for the sake of simplicity in filter implementation. In other words, we represent the effects of torque measurement and dynamic model error using additive noise in the process model.

In the prediction step, having determined the set of feet in contact using estimated contact forces, the mean is propagated using the discrete nonlinear process model. The discrete Jacobian of the process model, F_k , is computed and used to propagate the error covariance matrix. The prediction step is thus

$$\mu_k^- = f(\mu_{k-1}^+, u_{k-1}) \quad (15)$$

$$P_k^- = (F_{k-1} P_{k-1}^- F_{k-1}^T) + Q_k \quad (16)$$

where the minus superscript denotes the *a priori* (before measurement update) mean estimate, and the plus superscript denotes the *a posteriori* (after measurement update) mean estimate.

In the update step, the measurements are integrated into the EKF using the *a priori* estimates, the measurement noise

covariance, and the measurement itself as follows.

$$K_k = P_k^- H_k^T (H_k P_k^- H_k^T + R_k)^{-1} \quad (17)$$

$$\mu_k^+ = \mu_k^- + K_k (z_k - H_k \mu_k^-) \quad (18)$$

$$P_k^+ = (I - K_k H_k) P_k^- \quad (19)$$

B. Discrete, Nonlinear Model

In the prediction step, we need to propagate the mean of the state using the discretized nonlinear process model. We discretize the dynamics by applying the first-order Euler integration method to the nonlinear process model (11), yielding the following.

$$\mu_k^- = \begin{bmatrix} c_{k-1} \\ l_{k-1} \\ k_{k-1} \end{bmatrix} + \begin{bmatrix} \frac{1}{m} l_{k-1} \Delta t \\ [A\tau + b] \Delta t \end{bmatrix} \quad (20)$$

C. Discrete, Linear Model

We need the discretized, linear dynamics in order to propagate the state covariance matrix. By preference, first we linearize the dynamics and then discretize them at the filtering frequency. Since our nonlinear model for the momentum states $[l, k]^T$ is expressed implicitly as a function of the vectors of generalized positions and velocities, we compute the continuous Jacobian of (9) using finite differencing to find the corresponding entries of F_c . By considering small variations of q and v around their current values, denoted $q^+ = q \oplus \delta q$ and $v^+ = v + \delta v$, we have

$$\frac{\Delta \dot{h}_G}{\Delta c} = \frac{\dot{h}_G(q^+, v, \tau) - \dot{h}_G(q, v, \tau)}{g(q^+) - g(q)} \quad (21)$$

$$\frac{\Delta \dot{h}_G}{\Delta l} = \frac{\dot{h}_G(q^+, v^+, \tau) - \dot{h}_G(q, v, \tau)}{l(q^+, v^+) - l(q, v)} \quad (22)$$

$$\frac{\Delta \dot{h}_G}{\Delta k} = \frac{\dot{h}_G(q^+, v^+, \tau) - \dot{h}_G(q, v, \tau)}{k(q^+, v^+) - k(q, v)} \quad (23)$$

where c , l , k , and \dot{h}_G are calculated using (12), (6), and (7), respectively. Note that we use \oplus when perturbing the generalized coordinates because $q \in SE(3) \times \mathbb{R}^n$. The continuous prediction Jacobian matrix is then

$$F_c = \begin{bmatrix} 0_{3 \times 3} & \frac{1}{m} I_{3 \times 3} & 0_{3 \times 3} \\ \left[\frac{\Delta \dot{h}_G}{\Delta c} \right] & \left[\frac{\Delta \dot{h}_G}{\Delta l} \right] & \left[\frac{\Delta \dot{h}_G}{\Delta k} \right] \end{bmatrix} \quad (24)$$

In the discrete form the Jacobian is truncated at first order for simplicity to yield $F_k \approx I_{9 \times 9} + F_c \Delta t$, and the discretized state covariance matrix is likewise approximated by $Q_k \approx F_k Q_c F_k^T \Delta t$.

The Jacobian of the measurement model in the update step is simply $H_k = I_{9 \times 9}$ since we measure the states directly, and finally the continuous measurement covariance matrix is discretized as $R_k \approx \frac{R_c}{\Delta t}$.



Fig. 1: Snapshots of the first motion scenario (moving the base while balancing).

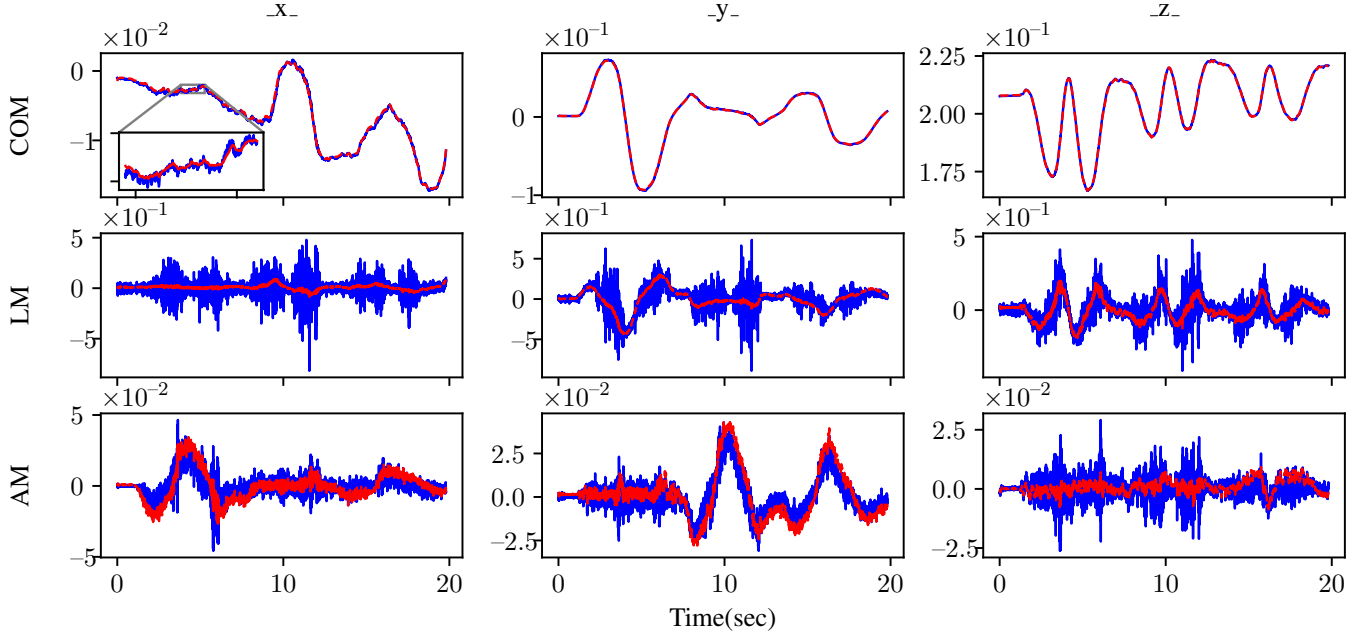


Fig. 2: Motion #1: Rotation of the base with all feet in contact. Estimation of the CoM (m) (top row), linear momentum ($\frac{kgm}{s}$) (middle row) and angular momentum ($\frac{kgm^2}{s}$) (bottom row). Columns denote x,y, and z values.

D. Observability Analysis

The process model of the proposed estimator is a highly-nonlinear function of the states; in general, we may investigate the observability of a nonlinear estimator by forming the nonlinear observability matrix [19]. Given a system with nonlinear process model $\dot{x} = f(x)$ and measurement model $y = h(x)$, the nonlinear observability matrix is

$$O = \begin{bmatrix} \nabla h(x) \\ \nabla(\nabla h \bullet f(x)) \\ \nabla(\nabla(\nabla h \bullet f(x)) \bullet f(x)) \\ \vdots \end{bmatrix}$$

where ∇ denotes the Jacobian with respect to x . The state of the estimator is observable if O has full rank.

In our case, the process model cannot be expressed explicitly in terms of the states, preventing us from computing Jacobians of $f(x)$. However, because we directly measure the full state, we have $\nabla h(x) = H_k = I_{9 \times 9}$. This already means that O has full column rank, so the state is observable. This is in agreement with the results of [10], where O is computed for a similar momentum estimator. The difference in this case is that higher-order terms would depend not on measured contact wrenches, but instead on properties of the constrained dynamics model and on measured generalized positions and velocities. As in those results, since we directly measure the state, higher-order terms do not affect observability (O cannot lose rank).

IV. RESULTS

In this section, we present the experimental results of performing estimation of the centroidal states both with and without the use of torque measurements, for a variety of different gaits on the quadruped robot Solo12 [13]. Specifically, we consider three different behaviors: moving the base while balancing, trotting, and jumping. The trajectories are generated using the trajectory optimization framework in [20], and the whole-body controller in [13] is used to track these trajectories while satisfying friction cone constraints. Note that we do not close the control loop around the estimated centroidal states; this is left to future work.

A. Motion #1: moving the base while balancing

The first scenario we consider is a motion in which we move the base without any contact switching (Fig. 1). The main goal of this test is to evaluate the quality of the estimated states in isolation from uncertainties introduced by contact switching as well as contact detection. Fig. 2 shows the centroidal states computed from (6) and forward kinematics (blue) compared against the estimated states from our proposed torque measurement-based EKF (red). The use of torque measurements in the proposed EKF is seen to significantly filter the centroidal momentum without adding delays.



Fig. 3: Snapshots of the second motion scenario (forward trotting).

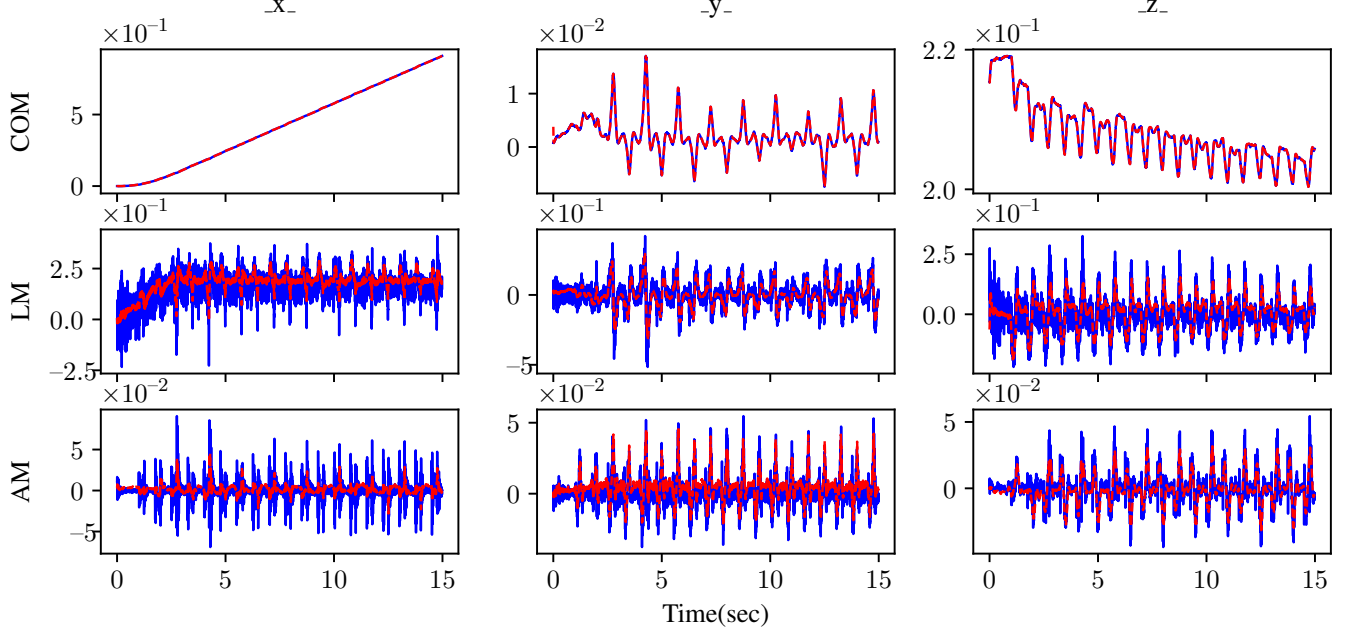


Fig. 4: Motion #2: Forward trotting with contact switching. Estimation of the CoM (m) (top row), linear momentum ($\frac{kgm}{s}$) (middle row) and angular momentum ($\frac{kgm^2}{s}$) (bottom row). Columns denote x,y, and z values.

B. Motion #2: forward trotting

In the second scenario, we consider a more complex motion involving intermittent contact switching. In this test, the robot moves forward approximately one meter in a trotting gait (Fig. 3). Contact detection is performed by projecting the joint torques of each leg through the Jacobian into the space of endeffector forces, and applying a force threshold to determine whether each foot is in contact. As shown in Fig. 4, in this case there are large discontinuities in the computed states (blue) due to the contact switches; in practice, these anomalies could destabilize a control loop if these states are used for feedback. However, the proposed torque measurement-based EKF (red) is seen to reduce the magnitude of these discontinuities, resulting in state estimates which are more suitable for use in a control loop.

C. Motion #3: jump in place

The third motion we consider is a jump in place (Fig. 5). This motion is especially challenging, as there is considerable impact during landing that could be problematic if a direct force/torque sensor at the end-effector were used to estimate the centroidal states as was done in [10]. However, since we are instead using torque measurements in the proposed estimator, we benefit from the fact that Solo12's structural and drive system damping filters out the effect of the impact from measured torque considerably. This helps prevent the estimator from diverging in the presence of large

impacts. As demonstrated by the results shown in Fig. 6, the proposed estimator is not significantly affected by the impact force during landing, and can thus filter out the measurement noise even in the presence of large impact forces during dynamic maneuvers.

V. CONCLUSIONS AND FUTURE WORK

In this paper, we proposed an approach to use joint torque measurements in the centroidal state estimation procedure for legged robots. To obtain the relationship between the joint torques and centroidal states, we projected the whole-body dynamics of the robot into the nullspace of the contact constraints. Then, we used the resulting equations as the process model of an EKF with joint torque input to estimate the centroidal states. We evaluated the performance of the resulting estimator for three different gaits on the quadruped robot Solo12. The results of these experiments showed that the estimated states from our approach have considerably less noise when compared to the naive computation of the centroidal states from the measured encoder values and estimated base states while maintaining minimal delay.

In the future, we would like to test the performance of closed-loop momentum control using the estimated centroidal states from the proposed EKF. Furthermore, we would like to mitigate the effects of dynamic model uncertainties by simultaneously estimating the centroidal states and performing online model identification. We are also interested

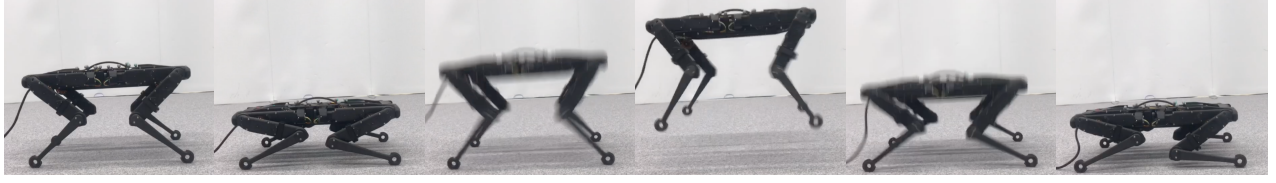


Fig. 5: Snapshots of the third motion scenario (jump in place).

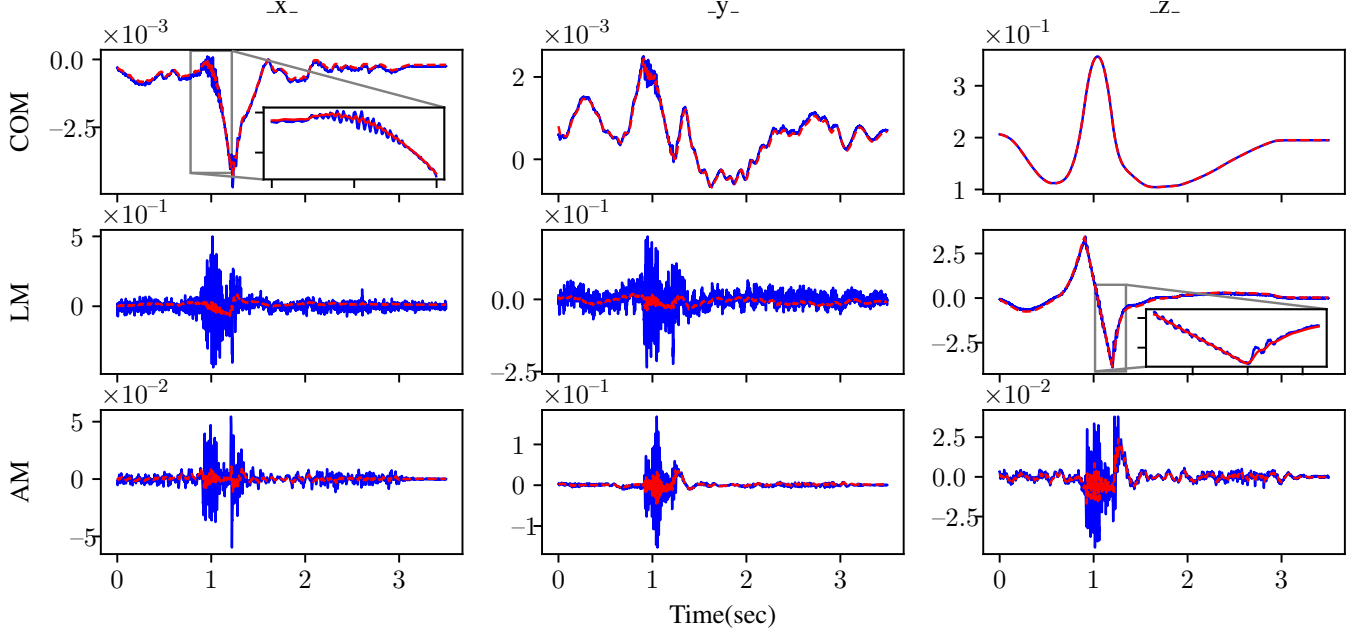


Fig. 6: Motion #3: Jump in place with contact switching. Estimation of the CoM (m) (top row), linear momentum ($\frac{kgm}{s}$) (middle row) and angular momentum ($\frac{kgm^2}{s}$) (bottom row). Columns denote x,y, and z values.

in extending the estimation problem to enable identification of the (non-rigid) contact model parameters, which could be used to adapt the controller when the surface properties are changed.

REFERENCES

- [1] M. Bloesch, M. Hutter, M. A. Hoepflinger, S. Leutenegger, C. Gehring, C. D. Remy, and R. Siegwart, "State estimation for legged robots-consistent fusion of leg kinematics and imu," *Robotics*, vol. 17, pp. 17–24, 2013.
- [2] N. Rotella, M. Bloesch, L. Righetti, and S. Schaal, "State estimation for a humanoid robot," in *2014 IEEE/RSJ International Conference on Intelligent Robots and Systems*, pp. 952–958, IEEE, 2014.
- [3] M. F. Fallon, M. Antone, N. Roy, and S. Teller, "Drift-free humanoid state estimation fusing kinematic, inertial and lidar sensing," in *2014 IEEE-RAS International Conference on Humanoid Robots*, pp. 112–119, IEEE, 2014.
- [4] M. Fourmy, T. Flayols, P.-A. Léziart, N. Mansard, and J. Solà, "Contact forces preintegration for estimation in legged robotics using factor graphs," in *2021 IEEE International Conference on Robotics and Automation (ICRA)*, pp. 1372–1378, IEEE, 2021.
- [5] R. Hartley, M. Ghaffari, R. M. Eustice, and J. W. Grizzle, "Contact-aided invariant extended kalman filtering for robot state estimation," *The International Journal of Robotics Research*, vol. 39, no. 4, pp. 402–430, 2020.
- [6] M. Camurri, M. Ramezani, S. Nobili, and M. Fallon, "Pronto: A multi-sensor state estimator for legged robots in real-world scenarios," *Frontiers in Robotics and AI*, vol. 7, p. 68, 2020.
- [7] N. Rotella, S. Schaal, and L. Righetti, "Unsupervised contact learning for humanoid estimation and control," in *2018 IEEE International Conference on Robotics and Automation (ICRA)*, pp. 411–417, 2018.
- [8] G. Bledt, P. M. Wensing, S. Ingersoll, and S. Kim, "Contact model fusion for event-based locomotion in unstructured terrains," in *2018 IEEE International Conference on Robotics and Automation (ICRA)*, pp. 4399–4406, IEEE, 2018.
- [9] G. Valsecchi, R. Grandia, and M. Hutter, "Quadrupedal locomotion on uneven terrain with sensorized feet," *IEEE Robotics and Automation Letters*, vol. 5, no. 2, pp. 1548–1555, 2020.
- [10] N. Rotella, A. Herzog, S. Schaal, and L. Righetti, "Humanoid momentum estimation using sensed contact wrenches," in *2015 IEEE-RAS 15th International Conference on Humanoid Robots (Humanoids)*, pp. 556–563, IEEE, 2015.
- [11] M. Hutter, C. Gehring, D. Jud, A. Lauber, C. D. Bellicoso, V. Tsounis, J. Hwangbo, K. Bodie, P. Fankhauser, M. Bloesch, *et al.*, "AnyMal-a highly mobile and dynamic quadrupedal robot," in *2016 IEEE/RSJ international conference on intelligent robots and systems (IROS)*, pp. 38–44, IEEE, 2016.
- [12] B. Katz, J. Di Carlo, and S. Kim, "Mini cheetah: A platform for pushing the limits of dynamic quadruped control," in *2019 International Conference on Robotics and Automation (ICRA)*, pp. 6295–6301, IEEE, 2019.
- [13] F. Grimmering, A. Meduri, M. Khadiv, J. Viereck, M. Wüthrich, M. Naveau, V. Berenz, S. Heim, F. Widmaier, T. Flayols, *et al.*, "An open torque-controlled modular robot architecture for legged locomotion research," *IEEE Robotics and Automation Letters*, vol. 5, no. 2, pp. 3650–3657, 2020.
- [14] M. Chignoli, D. Kim, E. Stanger-Jones, and S. Kim, "The mit humanoid robot: Design, motion planning, and control for acrobatic behaviors," in *2020 IEEE-RAS 20th International Conference on Humanoid Robots (Humanoids)*, pp. 1–8, IEEE, 2021.
- [15] "Agility robotics cassie." <https://www.agilityrobotics.com/robots/#cassie>.
- [16] E. Daneshmand, M. Khadiv, F. Grimmering, and L. Righetti, "Variable horizon mpc with swing foot dynamics for bipedal walking control," *IEEE Robotics and Automation Letters*, vol. 6, no. 2, pp. 2349–2356, 2021.

- [17] M. Mistry and L. Righetti, "Operational space control of constrained and underactuated systems," *Robotics: Science and systems VII*, pp. 225–232, 2012.
- [18] D. E. Orin and A. Goswami, "Centroidal momentum matrix of a humanoid robot: Structure and properties," in *2008 IEEE/RSJ International Conference on Intelligent Robots and Systems*, pp. 653–659, IEEE, 2008.
- [19] R. Hermann and A. J. Krener, "Nonlinear controllability and observability," *Automatic Control, IEEE Transactions on*, vol. 22, pp. 728–740, Oct 1977.
- [20] B. Ponton, M. Khadiv, A. Meduri, and L. Righetti, "Efficient multicontact pattern generation with sequential convex approximations of the centroidal dynamics," *IEEE Transactions on Robotics*, vol. 37, no. 5, pp. 1661–1679, 2021.